Iraqi Geological Journal

Journal homepage: https://www.igj-iraq.org

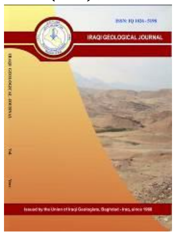

Application of the Water Quality Index Model for Groundwater Quality Assessment in the Dibdiba Aquifer, South of Iraq

Huda S. Abdulameer[1*] and Wasan S. Al-Qurnawi[1]

[1] Department of Geology, College of Science, University of Basrah, Basrah, Iraq

[*] **Correspondence**:hudasalih137@gmail.com

Received: 20 March 2025
Accepted: 3 July 2025
Published: 30 September 2025

Abstract

This study evaluates the Groundwater Quality Index of the Dibdiba Aquifer in the Zubair-Safwan area of southern Iraq. A total of 264 groundwater samples were analyzed over 24 years (2000-2024), divided into three temporal intervals (2000-2007, 2008-2015, and 2016-2024), to assess spatial and temporal variations in water quality. Eleven physicochemical parameters were measured, including pH, Total Dissolved Solids, Electrical Conductivity, major cations (calcium Ca^{2+}, magnesium Mg^{2+}, sodium Na^{+}, potassium K^{+}), and anions (chloride Cl^{-}, sulfate SO_4^{2-}, bicarbonate HCO_3^{-}, and nitrate NO_3^{-}), using standard analytical techniques (ICP-MS, UV-visible spectrophotometry, and ion chromatography). The results reveal a progressive decline in groundwater quality over time. A 10% reduction in Groundwater Quality Index values was observed between the first and second periods, while the third period showed a marked deterioration, with many samples exceeding Groundwater Quality Index values of 300. Spatially, the southwestern zone showed the best groundwater quality (Groundwater Quality Index: 17-104), indicating good to excellent suitability. In contrast, the northeastern, central, and eastern areas ranged from poor to very poor quality (Groundwater Quality Index: 104-300), with some spots exceeding 300, making the water unsuitable for drinking by WHO standards. The increase in Groundwater Quality Index values is primarily attributed to elevated concentrations of SO_4^{2-}, Cl^{-}, Mg^{2+}, Na^{+}, and TDS. These findings emphasize the urgent need for groundwater treatment and integrated management strategies to ensure sustainable water use in the region.

Keywords: Groundwater quality; Dibdiba aquifer; Southern Iraq; Water quality index WQI; Water quality assessment

1. Introduction

The Zubair and Safwan region, located in southern Basra Governorate, is agriculturally significant and heavily reliant on groundwater resources, primarily sourced from the Dibdiba aquifer. Given the region's arid climate, limited precipitation, and increasing anthropogenic pressures, groundwater has become a vital component for sustaining agriculture and supporting human livelihoods. In light of growing concerns regarding groundwater quality degradation, this study employs the Groundwater Quality Index (GWQI) to assess the suitability of water for domestic and agricultural uses. GWQI is a comprehensive scoring system that provides an overall assessment of water quality by integrating several physicochemical parameters. It is especially effective in evaluating groundwater usability for various purposes, including drinking, irrigation, and industrial applications (Reza and Singh, 2010). With the primary objective of evaluating the long-term temporal dynamics and fluctuations in groundwater quality, this study aims to provide a more refined understanding of the evolution of water quality patterns over time. This approach facilitates the detection of significant changes in concentration levels and helps identify potential sources of contamination or degradation, whether driven by natural or anthropogenic factors. This research specifically focuses on the Dibdiba aquifer, which, like other aquifers within the Dibdiba Formation, has been increasingly affected by climate change. Although several studies have investigated groundwater quality in the region (Abdulameer and Al-Mallah, 2018) and others across Iraq have applied the GWQI model (Awadh et al., 2016; Fatah et al., 2020; Al-Dulaimi and Al-Kubaisi, 2022; Yashooa et al., 2024). This research presents the first comprehensive, longitudinal application of GWQI to the Dibdiba aquifer in southern Iraq. A total of 264 groundwater samples were collected between 2000 and 2024 and analyzed for 11 key physicochemical parameters**,** including physical properties **(**pH, Total Dissolved Solids (TDS), and Electrical Conductivity (EC), major cations **(**calcium (Ca^{2+}), magnesium (Mg^{2+}), sodium (Na^{+}), and potassium (K^{+})), and major anions **(**chloride (Cl^{-}), sulfate (SO_4^{2-}), bicarbonate (HCO_3^{-}), and nitrate (NO_3^{-})). Spatial and temporal analyses were conducted using Geographic Information System (GIS) tools and kriging interpolation techniques to visualize and quantify water quality variations across four distinct time intervals. This research provides valuable insight into the progressive deterioration of groundwater quality in the region. It also underscores the broader implications of climate change and anthropogenic activities on groundwater resources in arid and semi-arid environments. The findings emphasize the urgent need for sustainable groundwater management and treatment strategies to ensure safe and reliable water availability for future generations.

2. The Study Area

The Safwan-Zubair region is located in the southernmost part of Iraq, along the northeastern edge of the Arabian Gulf, within the administrative boundaries of Basrah Governorate. This study area covers approximately 3351 km², extending between latitudes 29°59′N and 30°29′N and longitudes 47°42′E and 47°58′E. The terrain is primarily flat with minor undulations, and elevation ranges from 21 m below sea level to about 135 m above sea level. Fig. 1 illustrates the geographical location and topographic characteristics of the area, derived from a 12.5 m resolution Digital Elevation Model (DEM) obtained from the Alaska Satellite Facility Distributed Active Archive Center (ASF DAAC).

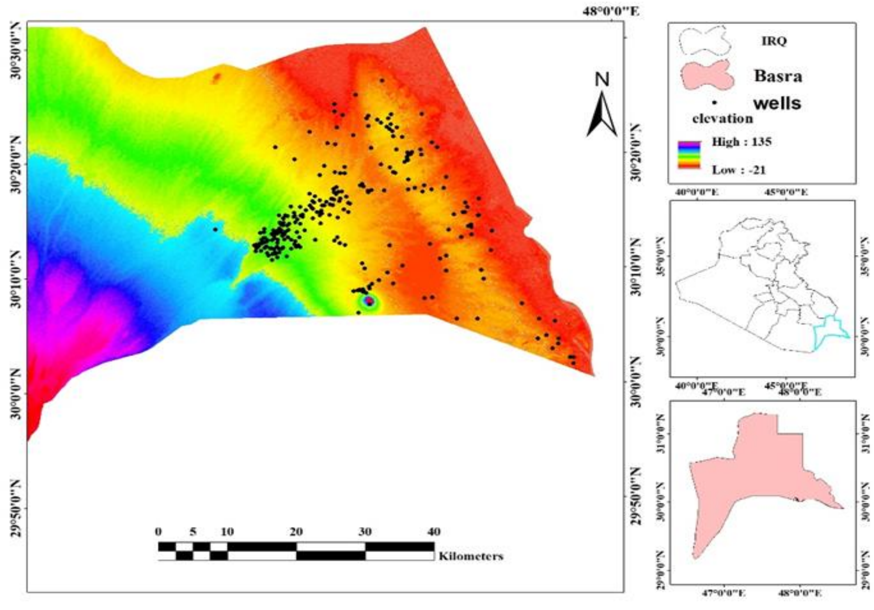

Fig. 1. The study area, elevation, and well location

Climatically, the region falls within the arid to semi-arid zone, characterized by long, extremely hot summers with temperatures often exceeding 50°C and mild winters. The average annual precipitation is relatively low, around 150 mm, with most rainfall occurring between November and March. High evaporation rates and prolonged dry periods contribute to substantial stress on groundwater resources, which serve as the primary source of water due to the scarcity of surface water in the region. Additionally, the region's proximity to the Arabian Gulf increases relative humidity during the warmer months, influencing evapotranspiration rates and the moisture dynamics of shallow soils. These environmental and climatic conditions significantly impact both the spatial distribution and quality of groundwater, which is essential for domestic, agricultural, and industrial purposes. Land use in the Safwan-Zubair area is predominantly agricultural, making it vital to understand the interaction between topographic, climatic, and hydrological factors for developing accurate models for groundwater storage management, especially in arid and semi-arid environments.

The Safwan-Zubair region, located in the extreme southern part of Iraq, lies within the Arabian Plate and is structurally situated in the Mesopotamian Foredeep Basin. This area is characterized by relatively flat topography and is geologically dominated by Tertiary and Quaternary sediments, which have been shaped by prolonged tectonic, depositional, and erosional processes (Al-Sudani, 2019). Fig. 2 illustrates the main geological units and sedimentary environments within the study area, highlighting its geological complexity. In the central and western sectors, the landscape is predominantly composed of polygenetic deposits, indicating the cumulative effect of multiple sedimentary processes over extended geological time scales. A prominent feature within this zone is the Sanam Plug, marked in red on the map, which represents a significant geological landmark influencing the surrounding deposits. To the northeast, near Basra and Zubair, the terrain is characterized by inland and estuarine sabkha deposits, reflecting arid climatic conditions with high evaporation rates and shallow, saline groundwater. These evaporitic environments are particularly important in understanding local groundwater salinity and soil chemistry. The region also exhibits a northeastward sedimentary transition, reflecting deltaic influences associated with the Dibdibba Formation, which was likely deposited in a deltaic to marginal marine setting (Jassim and Goff, 2006). The presence of mud lenses within these deposits suggests deposition under low-energy, possibly confined or semi-confined, conditions. The Quaternary sediments in the region, especially those from the alluvial fan, are found to overlie the Dibdibba Formation in certain areas, indicating episodic fluvial activity. The southern margin of the study area features a prominent alluvial fan system with a radial sediment dispersal pattern, indicating episodic or seasonal sediment influx from upstream wadi systems. In the southeastern and eastern zones, the geomorphology displays extensive tidal flat deposits, as evidenced by the presence of tidal channel formations connected to Khor Al-Zubair and its branching channels. These features are shaped by both horizontal and vertical erosion processes driven by tidal activity (Al-Muslih, 2012). Additionally, floodplain deposits from the Shatt Al-Basra and Euphrates rivers, along with dry marsh and freshwater lake sediments, are widely distributed across the region, adding to the stratigraphic complexity of the Quaternary cover. These deposits reflect both past and present hydrological dynamics that play a role in shaping the region’s surface and subsurface geological framework. The southwestern section of the study area features aeolian deposits and sand sheets sculpted by the dominant wind patterns, underscoring the role of wind in shaping desert surface geology. These wind-driven features, along with the diverse depositional environments, contribute to the heterogeneity of the subsurface and directly affect groundwater storage, movement, and quality. In summary, the Safwan-Zubair area exhibits a geologically diverse and dynamic landscape influenced by a combination of fluvial, aeolian, tidal, and evaporitic processes. Understanding these geological characteristics is essential for evaluating aquifer properties and effectively managing groundwater resources in the region.

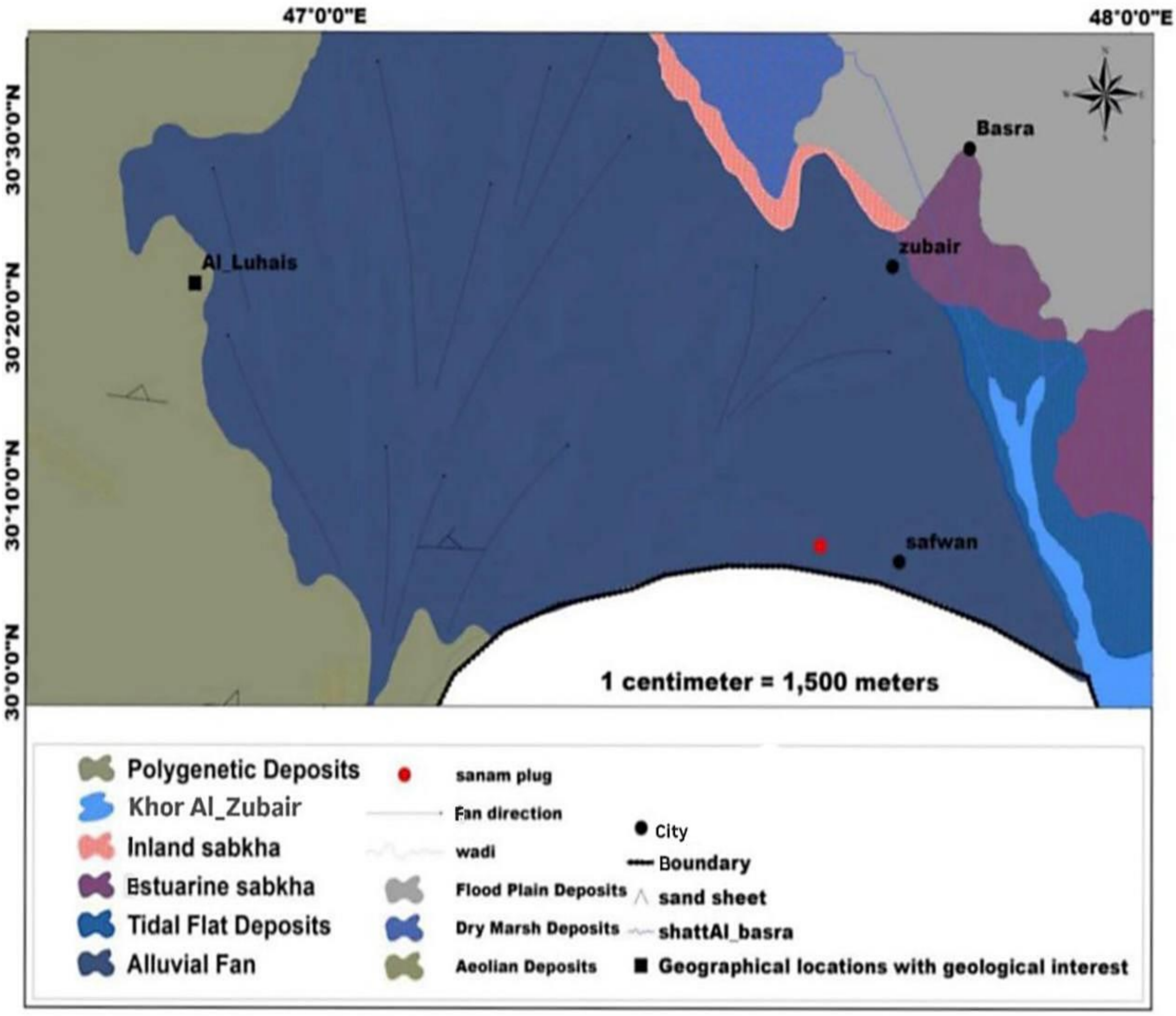

Fig. 2. Geological map of the study area (Source: Al-Sudani, 2019) modified by the author

3. Materials and Methods

3.1. The Climate Elements Impact

To evaluate the influence of climatic factors in the study area, climate data covering the period from 2000 to 2024 were collected from multiple sources, including the Climate and Scientific Research Center (C.S.R.C.), the General Authority for Meteorological and Seismic Monitoring in Baghdad, and the National Aeronautics and Space Administration (NASA) and Prediction of Worldwide Energy Resource (POWER), Data Access Viewer. The NASA POWER platform is an online tool that provides satellite-based global climate data. It offers a wide range of meteorological parameters, such as temperature, humidity, solar radiation, and wind speed, which are essential for climate analysis and environmental research. This tool enables users to retrieve both historical and recent climate data for any geographic location, thereby supporting comprehensive assessments of long-term climatic trends and their potential impacts on groundwater quality in arid and semi-arid regions. The spatial distribution and visualization of these climatic variables were conducted using GIS techniques, enabling accurate spatial analysis and the generation of thematic maps that illustrate climatic variability across the study area. A summary of the collected climate data is presented in Table 1.

Table 1. Monthly and annual average meteorological data for the study area (2000-2024)

Months	Rainfall (mm)	Temperature (°C)	Relative humidity %	Wind speed (m/s)
Jan	26.8	10.8	65.9	4.3
Feb	16.9	13.2	55.7	4.5
Mar	15.7	17.8	45.3	4.9
Apr	11.2	23.3	37.2	4.9
May	3.3	28.8	25.7	4.6
Jun	0.1	31.7	19.5	5.7
Jul	0.1	33.2	20.3	5.6
Aug	0.2	32.5	22.4	4.8
Sep	0.1	29.3	25.5	4.3
Oct	5.9	24.3	36.5	3.4
Nov	15.7	17.3	53.2	3.8
Dec	23.2	12.4	65.2	3.9
Minimum	0.1	10.8	19.5	3.4
Maximum	26.7	33.2	65.9	5.7
Average	10.4	22.7	39.9	4.6

3.2. Groundwater Sampling and Analysis

A total of 264 groundwater samples were evaluated in this study, comprising 25 samples collected through recent fieldwork and 239 historical well records obtained from the General Authority for Groundwater in Basra. The wells were spatially distributed throughout the Safwan-Zubair area and were sampled during multiple campaigns conducted between 2000 and 2024. To ensure data integrity, standard groundwater sampling protocols were rigorously followed to prevent contamination during collection, storage, and transportation. In the laboratory, a comprehensive set of physicochemical parameters was analyzed to assess groundwater quality. These included pH, Electrical Conductivity (EC), (TDS), and major cations (Ca^{2+}, Mg^{2+}, Na^{+}, and K^{+}) measured using Inductively Coupled Plasma Mass Spectrometry (ICP-MS). Major anions (Cl^{-}, SO_4^{2-}, HCO_3^{-}, and NO_3^{-}) were determined using UV-visible spectrophotometry and ion chromatography, depending on the specific ion.

3.3. Study Design and Temporal Classification

This study spans 24 years, from 2000 to 2024. The study period was divided into three distinct time intervals: 2000-2007, 2008-2015, and 2016-2024. This segmentation was designed to help identify anomalies, track temporal shifts in groundwater quality parameters, and assess the progression or deterioration of critical hydrochemical indicators over time. Simultaneously, climatic variables, including precipitation, temperature, relative humidity, and wind speed, were categorized into the same time intervals to assess their potential impact on groundwater quality. By analyzing the correlations between these climatic factors and variations in groundwater composition, the study aimed to investigate how climate change may have influenced temporal fluctuations in groundwater quality. The integration of both hydrochemical and climatic trends provided a comprehensive framework for detecting imbalances, understanding underlying causative factors, and guiding the development of effective groundwater management strategies within the study area.

3.4. Groundwater Quality Index

To synthesize multiple groundwater quality parameters into a single representative value, the GWQI was employed. This index offers a comprehensive assessment of water quality conditions across the study area and facilitates the identification of both spatial and temporal patterns. All parameters included in the GWQI calculation were subjected to statistical analysis, which involved determining the minimum, maximum, mean, and standard deviation values. Moreover, the measured concentrations were evaluated against the World Health Organization (WHO) standards for drinking water to assess potential health risks. This integrated methodological framework not only simplifies the interpretation of complex hydrochemical data but also enhances the understanding of long-term trends and possible sources of contamination. Consequently, the findings derived from the GWQI serve as a critical foundation for assessing the suitability of groundwater for domestic and agricultural use while also informing strategies for the sustainable management of groundwater resources. The descriptive statistics for each parameter, based on annual averages, are presented in Table 2.

Table 2. Physicochemical parameters in the study area (2000–2024), compared with the WHO (2017) drinking water standards

Parameter	Unit	Min	Max	Mean	SD	WHO Standard (2017)
pH	-	6.67	8.6	7.49	0.27	6.5-8.5
TDS	mg/L	2190	18800	6165.62	2291.06	600
EC	µs/cm	8.26	76920	8478.13	5340.27	500
Ca^{2+}	mg/ L	6.1	1383	524.78	321.65	250
Mg^{2+}	mg/L	9.48	3663	327.21	519.10	50
Na^{+}	mg/L	85	3241	520.09	425.45	200
K^{+}	mg/L	5.8	1274	139.37	260.24	20
Cl^{-}	mg/L	465	7579	1922.99	1037.09	250
SO_4^{2-}	mg/L	4.2	6128	2061.32	999.61	250
HCO_3^{-}	mg/L	2	1983	341.38	272.36	500
NO_3^{-}	mg/L	1	210	15.45	28.04	50

3.5. GWQI Assessment Model

This research applied the entropy approach to compute the GWQI. For Yufeng and Fengxiang (2009), entropy is the measure of disturbance of a system. Deterioration of groundwater quality and changes in its hydrochemical characteristics are systematic and have multiple causes, including vegetation on the surface and regional climate change, which encompasses changes in rainfall and temperature increases. Additionally, subsurface factors significantly impact groundwater quality, particularly those related to recharge sources and the aquifer's lithology. Moreover, human activities, including the misuse of water resources and excessive well drilling, further exacerbate these changes (Al-Ozeer and Al-Abadi, 2022).

The following are the main stages in determining weights using the entropy method:

The first stage includes the following three steps:

A: Normalization of the original evaluating matrix is a crucial step in assessing groundwater quality. This study's eleven physicochemical parameters (pH, TDS, EC, Ca^{2+}, Mg^{2+}, Na^{+}, K^{+}, Cl-, $SO_4^{-,}$ Hco_3^{-}, and No_3^{-}) were regarded as indications of groundwater appropriateness for drinking. Suppose (m) groundwater samples are taken to evaluate the chemical quality of an area. For each groundwater sample, (n) chemical components are analyzed (j = 1, 2, …, n). Based on the actual data, the value Matrix X can be built from actual data as:

$$x = \begin{bmatrix} x_{11} & x_{21} & x_{1n} \\ x_{21} & x_{22} & x_{2n} \\ x_{m1} & x_{m2} & x_{mn} \end{bmatrix}, \quad (1)$$

A standardization mechanism is essential to render the data dimensionless, thereby facilitating the comparison of chemical constituents across different parameters. According to Shi-Fei and Zhong-Zhi (2005), this process is essential when dealing with cost-type parameters, where larger values are considered more favorable. For such parameters, the standardization formula can be expressed as follows.

$$yi = \frac{x_i - x_{i(min)}}{x_{i(max)} - x_{i(min)}}, \quad (2)$$

While for the efficiency type (smaller values are better):

$$yi = \frac{x_{i(max)} - x_i}{x_{i(max)} - x_{i(min)}}, \quad (3)$$

Where:

i: Index or attribute.

xi: The original value of *i*.

$x_{i(\mathrm{max})}$,$x_{i(\mathrm{min})}$: Maximum and minimum values of original data.

Eqs. (2) and (3) normalize the data between 0 and 1. After the standardization process, the standard-grade matrix Y can be obtained.

$$y = \begin{bmatrix} y_{11} & y_{21} & y_{1n} \\ y_{21} & y_{22} & y_{2n} \\ y_{m1} & y_{m2} & y_{mn} \end{bmatrix}, \quad (4)$$

The index value ratio of the j index in (*i*) The sample is estimated as follows:

$$\mathrm{P_{ij}} = \frac{\mathrm{y_{ij}}}{\sum_{\mathrm{i=1}}^{\mathrm{m}} \mathrm{y_{ij}}}, \quad (5)$$

B: Definition of entropy. The concept of entropy of the (*j*) indicator is defined when an analysis involves (n) evaluation indicators and (m) evaluation objects. The following formula gives the information entropy:

$$e_j = -\frac{1}{ln\, m} \sum_{i=1}^{m} p_{ij}\ lnp_{ij}, \quad (6)$$

The smallest value of (e_j) is the largest effect of the *(j)* index

C: Definition of the entropy weight. The entropy weight of the *(j)* indicator is defined as:

$$w_{ij} = \frac{1 - e_j}{\sum_{j=1}^{n}(1 - e_j)}, \quad (7)$$

The second stage is to determine the quality rating scale (q_j) for each parameter of the groundwater quality. The (q_j) is calculated as:

$$q_j = \frac{C_j}{S_j} \times 100, \quad (8)$$

Where:

C_j Is the concentration of all chemical components in each groundwater sample (mg/l).

Sj Is the WHO standard (WHO, 2017).

q_j Is the quality rating

The third stage is to use the linear combination technique to calculate GWQI:

$$GWQI = \sum_{j=1}^{n} W_{ij}\ q_j \quad (9)$$

The WQI values are typically divided into five categories: excellent, good, poor, very poor, and unsuitable for human consumption (Sahu and Sikdar, 2008). The calculation procedure for WQI is explained in detail by several authors (Pradhan et al., 2001; Dwivedi and Patha, 2007; Asadi et al., 2007; Saeedi et al., 2010; Yidana and Yidana, 2010). Table 3 typically classifies computed WQI values into five categories.

Table 3. Groundwater quality classification by WQI (Source: Sahu and Sikdar, 2008)

WQI	Status
<50	Excellent water
50-100	Good water
100-200	Poor water
200-300	Very poor water
>300	Unfit for drinking purposes

3.6. Spatial Analysis

A comprehensive spatial analysis of groundwater quality parameters was performed using Geographic Information System (GIS) tools in ArcGIS 10.8. Spatial distribution maps were generated through geostatistical interpolation, specifically the Empirical Bayesian Kriging (EBK) method, which allows for enhanced accuracy in representing spatial variability. These maps provided a clear visualization of the spatial distribution patterns of various physicochemical parameters across the study area. The analyzed parameters included pH, EC, TDS, major cations Ca^{2+}, Mg^{2+}, Na^{+}, K^{+}, and major anions Cl^{-}, SO_4^{2-}, HCO_3^{-}, and NO_3^{-}. In addition to groundwater quality parameters, spatial distribution maps for selected climatic variables, such as precipitation, relative humidity, and wind speed, were also developed using GIS techniques. Meanwhile, temperature trends were represented using graphical curve plots generated in Microsoft Excel to highlight temporal variations across the study period. These climate-related visualizations supported the interpretation of spatiotemporal trends in groundwater quality by illustrating potential climatic influences. Particular emphasis was placed on the Safwan-Zubair region to enable a more focused and detailed assessment of groundwater quality dynamics in relation to both spatial variation and climate conditions within this key area.

4. Results and Discussion

4.1. Influence of Climatic Factors on Groundwater Quality

Water quality, both at the surface and underground, is impacted by climate factors due to integral and natural phenomena such as evapotranspiration, mining, and the water-sediment-rock interphase (Al Ramahi et al., 2024). Climate change over the years has greatly influenced the quality of groundwater in the area under observation, as the area has been subjected to extremely hot weather conditions, rising to as high as 50°C Fig. 3. Over time, a consistent increase in temperature has been documented, directly influencing groundwater quality by raising evaporation rates and altering the hydrochemical balance within the aquifer system. As a result of rising temperatures, a marked decline in rainfall has been observed over the years. Choosing 4 periods to represent the spatial distribution of rainfall in the study area to match the GWQI categories as shown in Figs. 4 and 5, with precipitation levels decreasing gradually. Fig. 4A represents the spatial distribution of the average annual rainfall from (2000-2024) with an average of 57 mm. Fig. 4 B represents the spatial distribution of the average annual rainfall period one (2000-2007) with an average of 61.5mm, Fig. 5 A represents the spatial distribution of the average annual rainfall period two (2008-2015) with an average of 51mm and Fig. 5 B represents the spatial distribution of the average annual rainfall third period (2016-2024) with an average of 47.5mm. The Fig. 5 B illustrate that rainfall rates decreased over the last 20 years by 20% This reduction in rainfall, which is an important source of recharge in the area, has significantly elevated salt concentrations within the groundwater reservoir besides the unmanaged discharge, which depletes the aquifer, all of that leading to a deterioration in water quality. Furthermore, the high evaporation rate in the area exacerbates these conditions by accelerating salt accumulation and promoting more intense chemical reactions within the groundwater system, further contributing to its degradation. However, humidity levels, a crucial factor in maintaining the soil's water balance, significantly affect groundwater recharge. As illustrated in Fig. 6 A, the western and central regions, characterized by low humidity, experience higher water loss rates, resulting in an increasing decline in groundwater levels and, consequently, an increase in salt concentrations. In contrast, regions with higher humidity, such as the eastern and northeastern parts of the study area, benefit from reduced evaporation rates, which helps to maintain better groundwater quality. On the other hand, wind plays an indirect yet significant role in groundwater degradation by accelerating evaporation and moisture loss. In hyper-arid desert environments, where wind regimes are particularly intense and persistent, these processes become more pronounced. The strong winds enhance surface evaporation and promote the mobilization and deposition of salts and fine sediments. Over decades, this leads to increased salinity and a higher concentration of dissolved solids in the soil, which may subsequently infiltrate into the groundwater system and deteriorate its quality. As Fig. 6 B illustrates, wind-induced evaporation further aggravates salt accumulation, exacerbating the salinity of groundwater and affecting its overall quality and usability.

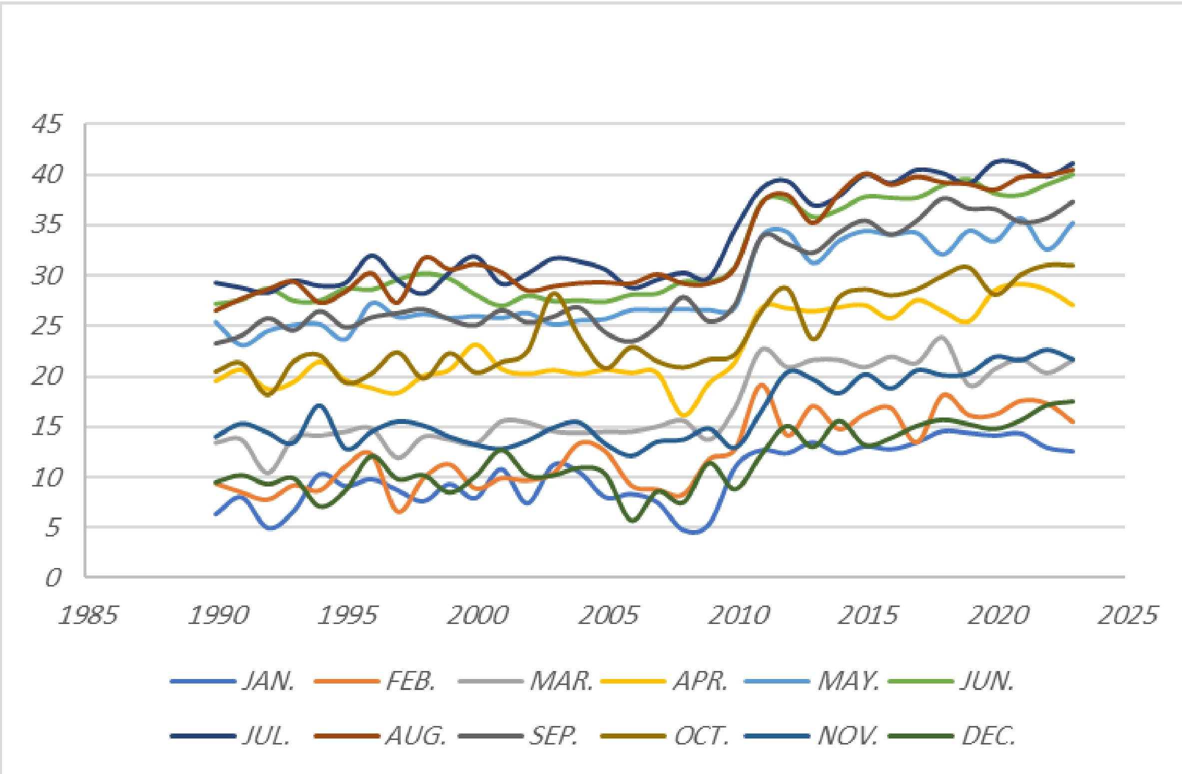

Fig. 3. The time series of temperature from 1990 to 2024

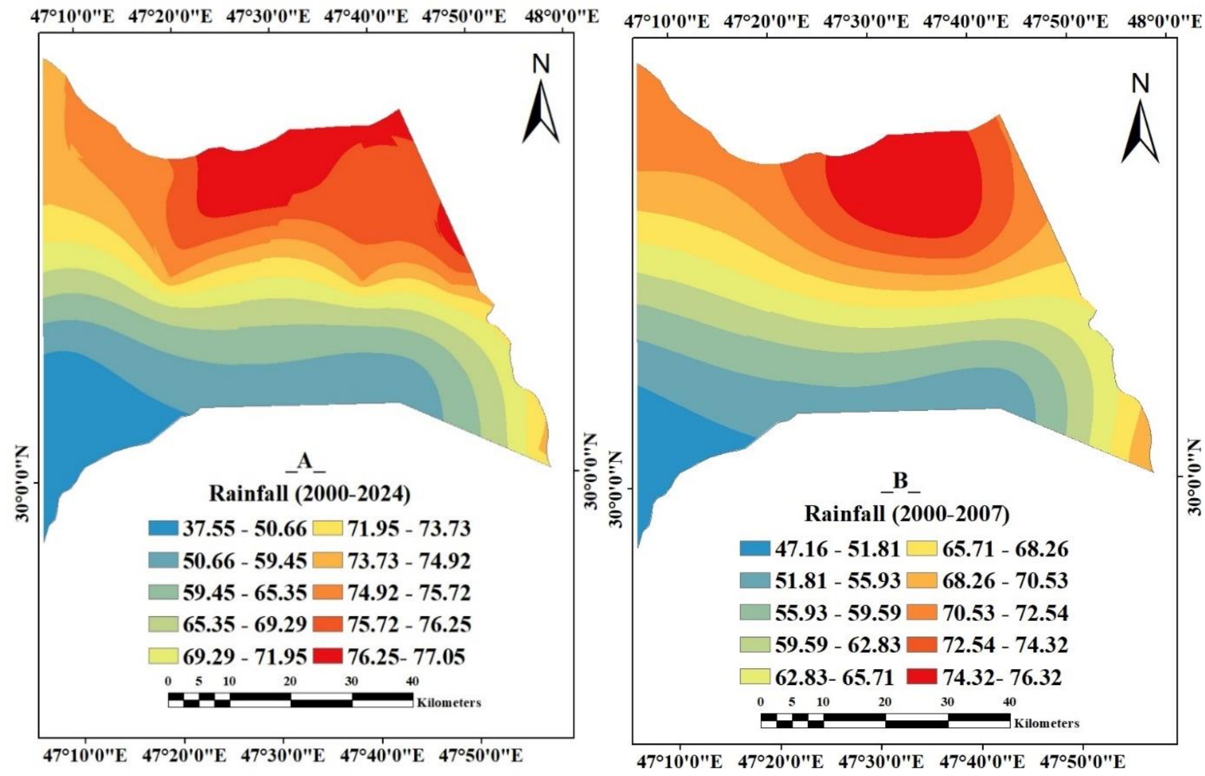

Fig. 4. Spatial distribution of average annual rainfall: (A) for the whole study duration (2000-2024); (B) for the baseline period (2000-2007), illustrating temporal variability in precipitation patterns

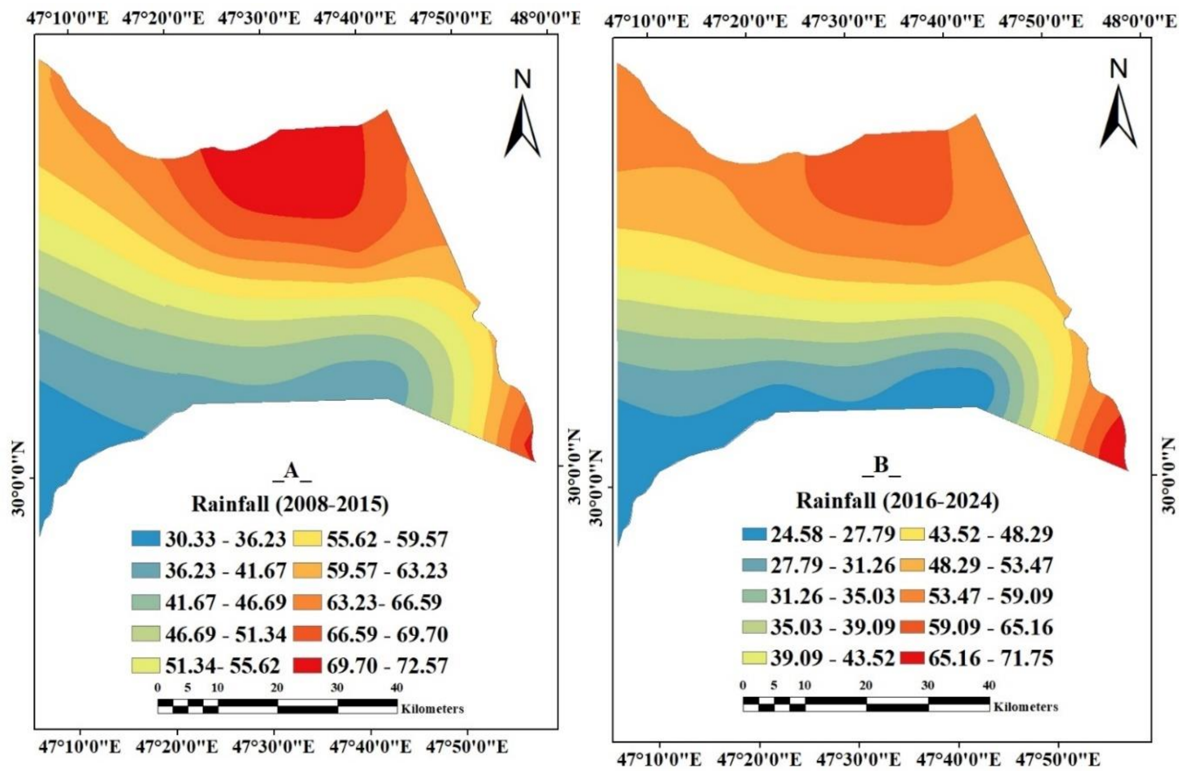

Fig. 5. Spatial distribution of average annual rainfall: (A) for the whole study duration (2008-2015); (B) for the baseline period (2016-2024), illustrating temporal variability in precipitation patterns

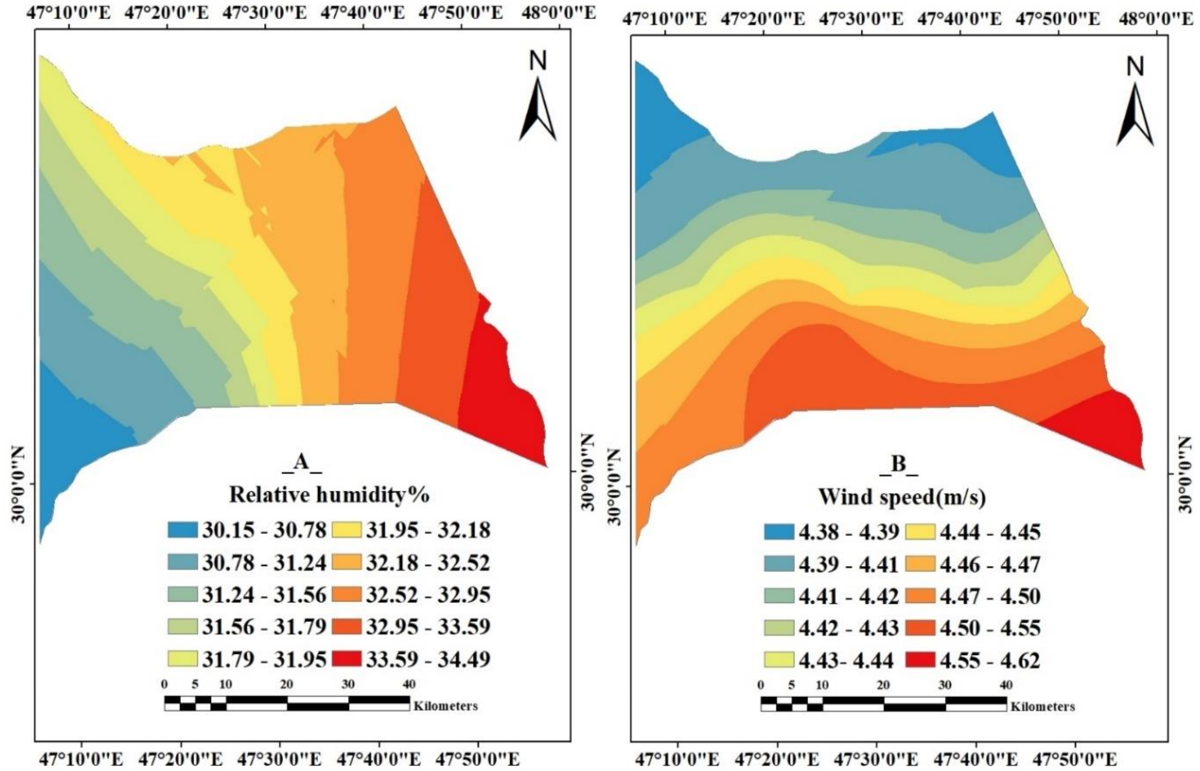

Fig. 6. Spatial distribution of the study area: (A) average annual relative humidity (2000-2024); (B) average annual wind speed (2000-2024)

4.2. Physicochemical Parameters Analysis

The spatial analysis of physicochemical parameters, including pH, TDS, EC, Ca^{2+}, Mg^{2+}, Na^{+}, Cl^{-}, K^{+}, SO_4^{2-}, HCO^{-}_3, and NO^{-}_3), was conducted on groundwater samples collected from the study area during the period from 2000 to 2024. The pH levels of the groundwater samples ranged from 7 to 8.5 throughout the study region. Elevated pH values, with measurements reaching up to 8.5, were predominantly observed in the central portion of the study area. These elevated values may be attributed to local ecological and hydrogeological settings in conjunction with the industrial activities situated west of the region. (Al-Qurnawi et al. 2024). On the other hand, the eastern portions of the study area had pH values between 6.5 and 7.5, which is largely a result of the mixing of fresh water and saline water from the Arabian Gulf. According to Table 2 and Fig.7A, the pH levels increase progressively to the west, which correlates with changes caused by geological and hydrological activities. The EC values of the samples tested from the region ranged from 8.26 μS/cm to 76,920 μS/cm, with an average of 8478 μS/cm. According to the WHO (2017), as shown in Table 2, the recommended limit for EC in drinking water is 500 μS/cm. The EC values in the study area are predominantly elevated, particularly in the southern, southeastern, and central regions. This increase is attributed to several factors, including the interaction between fresh and saline water from the Gulf, prolonged drought conditions, and intensive water use for irrigation purposes (Al-Qurnawy et al., 2024), as illustrated in Fig.7 B. The concentration of TDS in the groundwater of the study area ranged from 2,190 mg/l to 18,800 mg/l, with an average value of 6,165.62 mg/L, Table 2. The WHO (2017) indicates that the allowable limit of TDS in drinking water is 600 mg/l. As seen in Fig.8C, TDS concentrations were highest in the eastern and central parts of the study area, with a gradual decline observed toward the west. This spatial distribution likely reflects the combined influence of underlying geological formations and regional groundwater flow dynamics. (Awadh et al. 2016). Groundwater sodium Na^{+} concentration in the study area ranged from 85 mg/l to

3241 mg/l, with a mean value of 520.1 mg/l Table 2. The WHO (2017) suggests a limit of 200 mg/l for sodium in drinking water. An increased sodium concentration was observed in the western part of the study area, attributed to the region's dry climatic conditions. Higher levels of sodium concentration were also noticed in some eastern and central parts due to water interference and over-abstraction of groundwater, as Fig. 8D shows; these regions are more elevated than others. The content of Mg^{2+} in the groundwater from the study area was between 9.45 mg/l to 3,663 mg/l. The average was 327.2 mg/l, as shown in Table 2. (WHO, 2017) put forth a limit of 50 mg/l for magnesium in drinking water. In the area, magnesium concentrations were noted to rise in the northern and northwestern directions and also in the southeastern portions close to the Gulf. Overall, larger concentrations were noted in shallow saline irrigated areas and areas under the influence of waterlogging. These developments are shown in Fig. 9E. The range of concentrations of Ca^{2+} in the groundwater of the study region was 6.1 mg/l to 1,383 mg/l, whereas the average was 524.8 mg/l. (WHO, 2017) in the Table.2, provided a limit of 250 mg/l for calcium concentration in drinking water. The central and northwestern parts of the study area were found to have greater calcium concentrations than other regions, and this phenomenon could be due there climatic zones and irrigation schemes. Fig. 9 F shows the spatial variations during the study. The concentration of Cl^- in the groundwater ranged from 465 mg/l to 7579 mg/l, with an average of 1922.9 mg/l; Table 2. The WHO (2017) suggests that the maximum acceptable limit for chloride in drinking water is 250 mg/l. This suggests a need for concern in this region. The higher concentrations of chloride were found in the southeastern area of the region, mostly resulting from the combination of saltwater and freshwater (Al-Qurnawy et al., 2024). Moreover, this region is characterized by dry environmental conditions, which, along with the over-exploitation of groundwater resources, results in saltwater intrusion, which explains these concentrations. Fig. 10 G illustrates the chloride spatial concentrations. In the groundwater within the study area's boundaries, the concentration of SO_4^{2-} ranged between 4.2 mg/l and 6128 mg/l, with a mean value of 2061.3 mg/l; Table 2. The WHO, (2017)cites the recommended limit for sulfate in drinking water as 250 mg/l. Sulfate is affected by climatic conditions, water-soil interaction, and sulfate-bearing agricultural activity in the study area. Higher sulfate concentrations were noticed towards the eastern regions, where concentrations decreased westward. These spatial patterns are shown in Fig.10H. The concentration of HCO_3^- in the groundwater of the study area ranged from 2 mg/l to 1983 mg/l, with an average value of 341.41 mg/l; Table 2. The WHO (2017) recommends a limit of 500 mg/L for bicarbonate in drinking water. Geological and hydrological conditions influence bicarbonate concentrations, which were higher in the western parts of the study area, primarily due to climatic conditions, with a decrease towards the eastern parts. These spatial variations are illustrated in Fig. 11I. The (NO_3^-) concentration in the groundwater of the study area ranges from 1 mg/L to 210 mg/L, with an average concentration of 341.4 mg/L. The concentration of No^-_3 has recently been reconsidered due to its excessive levels in drinking water, so much so that the World (WHO, 2017) set a recommended limit of 50 mg/L. This resulted in various wells becoming supersaturated; some wells reached up to 125 mg/L, and others soared as high as 210 mg/L, all of which are in the Al-Zubair region. climatic and hydrological factors, as well as factors that can also affect the increase in nitrate levels. For instance, a most commonly known phenomenon is precipitation; its low levels tend to reduce the dilution, which therefore increases the accumulation of nitrates within the soil. Another example can be said that higher levels of evaporation tend to increase the concentration of salt and nitrates within the groundwater reservoirs. In addition, higher levels of water salinity tend to increase nitrate concentration as well, in turn leading to greater dissolution of the said compound (Ghalib, 2008). The concentration of nitrate is shown in detail in Fig.11 J.

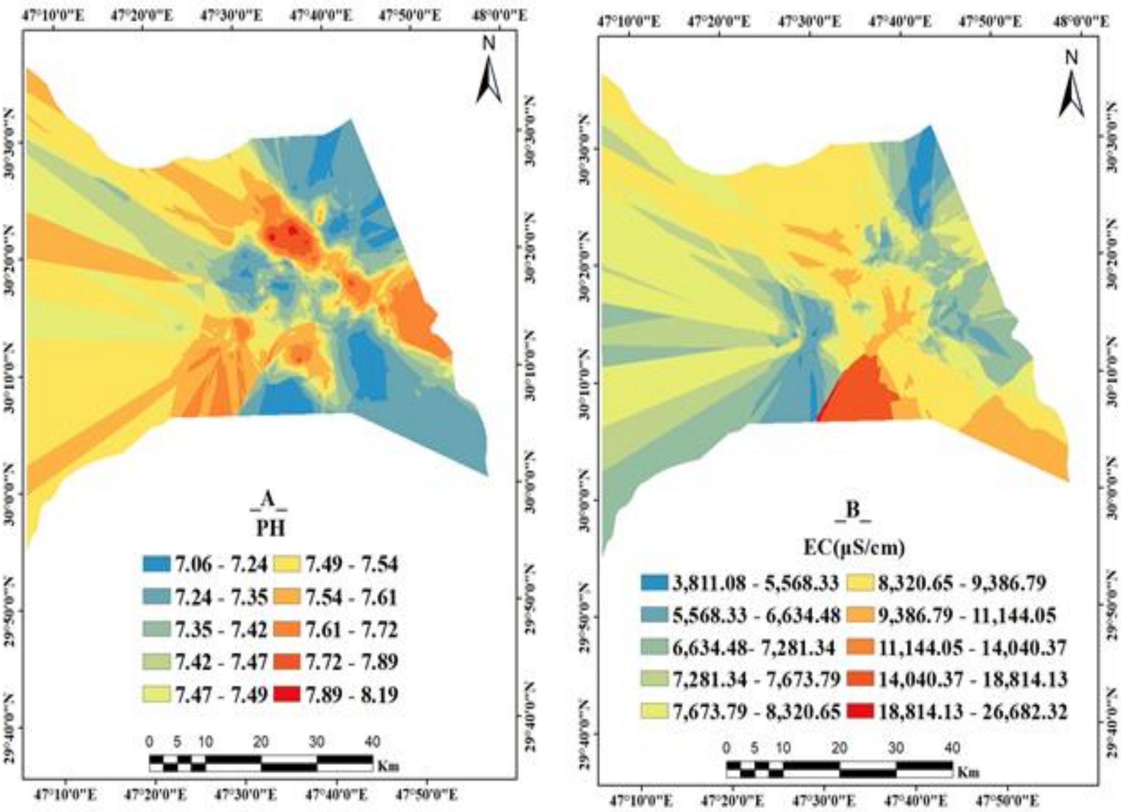

Fig. 7. Spatial distribution map for (A) PH, (B) EC of the study area

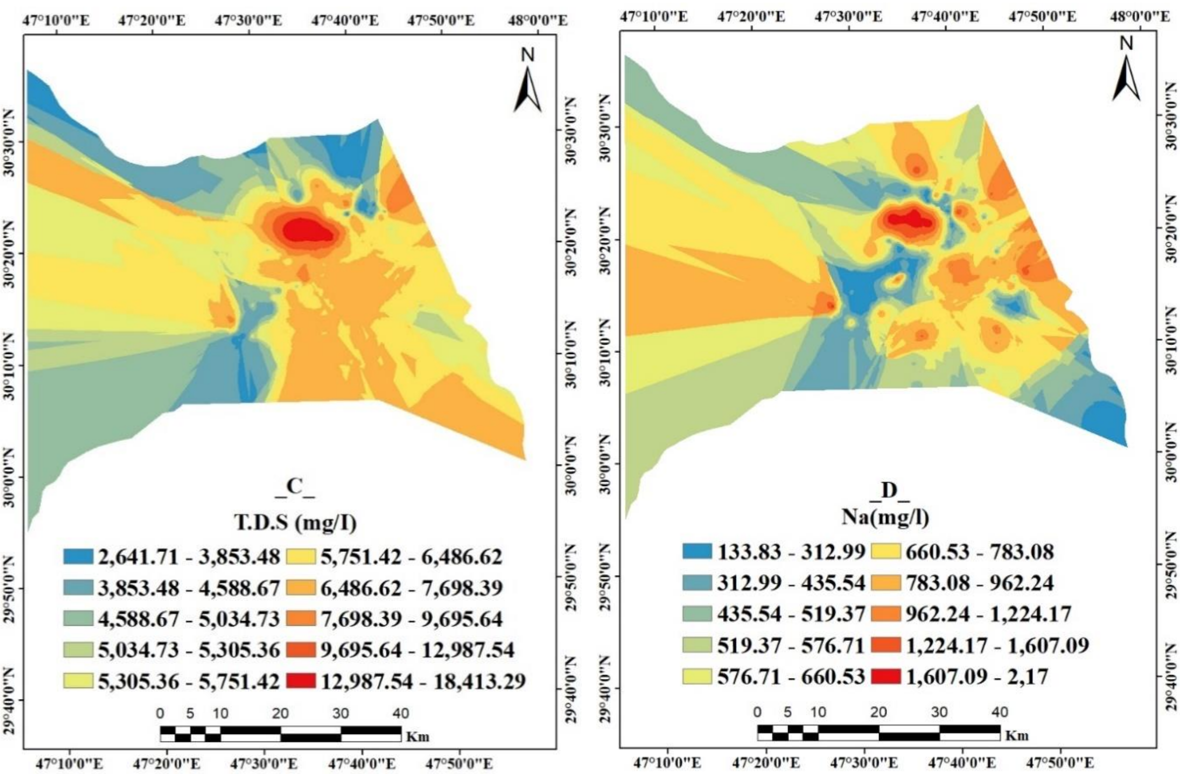

Fig. 8. Spatial distribution map for (C) TDS; (D) Sodium concentration of the study area

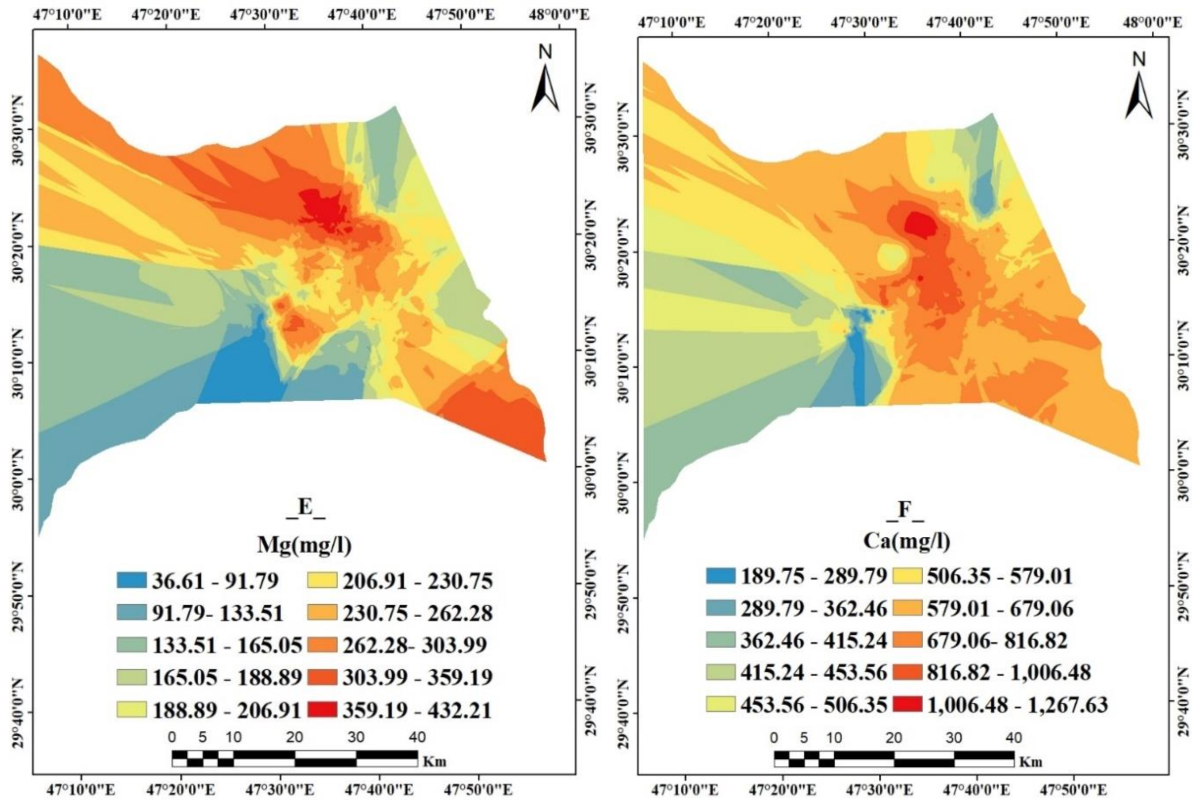

Fig. 9. Spatial distribution map for (E) Magnesium, (F) Calcium concentration of the study area

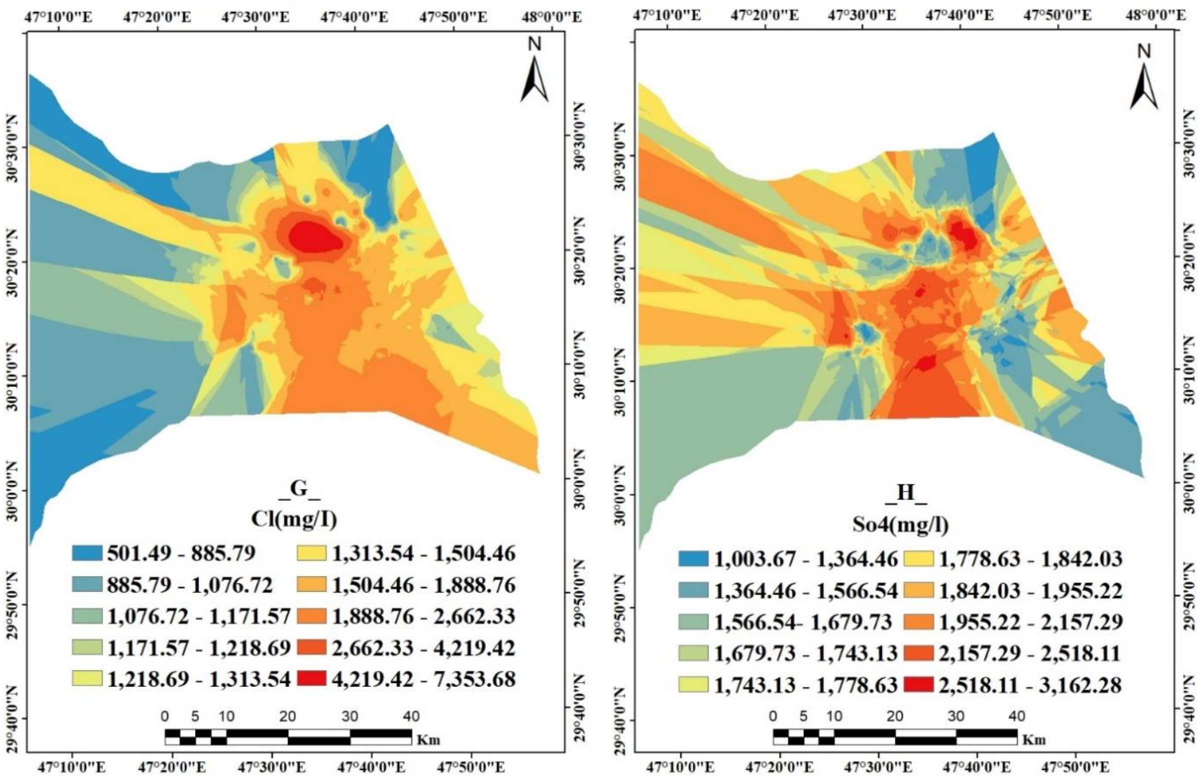

Fig. 10. Spatial distribution map for (G) Chloride, (H) Sulfate concentration of the study area

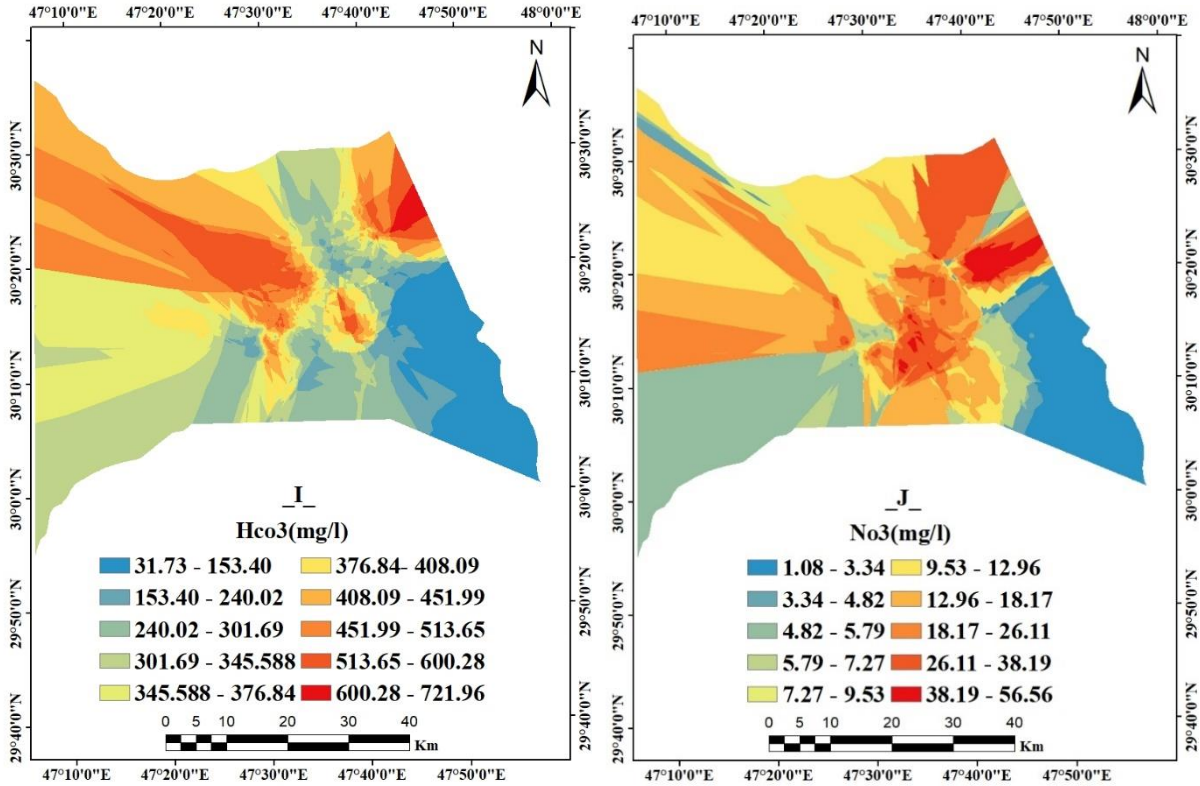

Fig. 11. Spatial distribution map for (I) Bicarbonate, (J) Nitrate concentration of the study area

4.3. Evaluation of GWQI in the Selected Study Region

The outcomes of this analysis provide valuable insights that support the assessment of groundwater quality in the region using the Groundwater Quality Index (GWQI). To effectively illustrate long-term spatial and temporal changes in water quality, the full study period (2000-2024) serves as a general reference frame for the analysis. Within this timeframe, data were further analyzed across three distinct temporal intervals, each spanning approximately eight years: 2000-2007, 2008-2015, and 2016-2024. This temporal segmentation facilitates the detection of evolving groundwater quality patterns and helps identify emerging trends, anomalies, and zones of degradation across the study area. The classification framework enabled a structured comparison of groundwater quality across time, allowing for the evaluation of both improvement and deterioration trends. The overall results for the full study period (2000-2024) reveal a significant decline in water quality across the region. During this general period, GWQI values in the southwestern parts of the study area ranged from 17 to 104, corresponding to classifications from excellent to good. In contrast, the northwestern, northeastern, and eastern zones were predominantly classified as poor to very poor, with GWQI values ranging from 104 to 300. The central and southern regions exhibited the most severe degradation, with GWQI values between 300 and 800, indicating water unfit for drinking (Table 3; Fig. 12).

The first temporal interval (2000–2007) was selected as the baseline period to assess groundwater quality deterioration at eight-year intervals up to the present. Table 4 represents the information entropy and weight results and provides a detailed assessment of groundwater quality during this time frame. It shows the study area classified as excellent water in the southwest parts, ranging from 37 to 53. While the north and center parts classified as good water range from 54 to 107, the poor water classification is located in the south, and some spots in the center part of the study area range from 108 to 146, Table 3; Fig.13, Rainfall during this period remained around the long-term average, supporting stable recharge conditions. Generally the number of discharges wells did not exceed 5000 in the area at that time, so the aquifer was not subject to depletion by pumping (Atiaa, 2000; Atiaa, 2007). A continued assessment of groundwater quality is presented in Table 5, which shows the information entropy and weight results for the period 2008-2015. During this interval, the study area was primarily classified as excellent in the southwestern parts and a small zone to the east, with GWQI values ranging from 26 to 51. In contrast, the northern, central, and southern parts were predominantly categorized as having good water quality, with ratings ranging from 52 to 107. A localized zone with comparatively higher GWQI values (108-114) was identified near Jabal Sanam, distinguishing it from the surrounding regions (Table 3; Fig. 14). Compared to the earlier period (2000-2007), only minor variations were observed in the chemical composition of groundwater. However, rainfall data from this period indicate a decline of approximately 18%, suggesting a gradual reduction in natural recharge rates. This reduction may have contributed to the subtle deterioration in water quality. Furthermore, the number of drilled wells had increased to 6,111 during this time, potentially reflecting a rise in groundwater consumption. The slight decline in GWQI values can, therefore, be attributed to both the limited recharge and the intensified rate of groundwater extraction, which may have contributed to aquifer depletion. Table 6 presents the information entropy and weight results for the final category, covering the period from 2016 to 2024. During this interval, the eastern parts of the study area were classified as having good water quality, with GWQI values ranging from 84 to 106. In contrast, poor water quality was predominant in the western and southwestern zones, ranging from 127 to 212. The most severely affected areas were located in the central and extreme southern regions, where GWQI values ranged between 212 and 334, classifying the water as very poor to unfit for drinking and thus unsuitable for human consumption (Table 3; Fig. 15). When compared with the baseline period (2000-2007), this phase recorded a further 20% decline in annual rainfall, which likely contributed to reduced recharge rates and the concentration of salts in the aquifer system. Additionally, according to the Basra Groundwater Authority (Al-Qurnawy et al., 2024), more than 12,000 wells were drilled in the region during this period. This significant increase in extraction contributed to aquifer depletion and seawater intrusion in the southern zones, both of which are reflected in the elevated GWQI values. The increase in GWQI values across many groundwater samples suggests that water in these areas is no longer suitable for direct consumption and now requires sustainable treatment before being used for drinking. A comparative analysis of groundwater quality across the three study periods indicated a progressive decline in water quality. Between the first (2000-2007) and second (2008-2015) periods, GWQI values suggested a moderate reduction in quality, estimated at around 10%. However, during the third period (2016-2024), a pronounced and sharp increase in GWQI values was recorded, indicating a substantial deterioration in groundwater quality. This marked shift reflects the cumulative impact of intensified groundwater abstraction, reduced natural recharge, and increasing salinity intrusion, particularly in the central and southern parts of the study area. These findings highlight the progressive degradation of groundwater quality across the study area, driven by both climatic stress and anthropogenic pressures. The spatial distribution of GWQI, as illustrated in Fig. 15, shows higher GWQI values in the eastern and southeastern zones, whereas the southwestern desert areas maintain relatively better water quality. This contrast is largely attributed to the lower intensity of human activities and the fact that the southwestern region serves as a major natural recharge zone for the Dibdiba aquifer. The temporal and spatial assessments are presented in Tables 3 through 6 and Figs. 15 through 18 provide a structured and integrated framework for groundwater quality monitoring. This framework clearly illustrates the growing challenges of salinization and aquifer depletion and underscores the urgent need for effective, adaptive groundwater management strategies in arid and semi-arid environments.

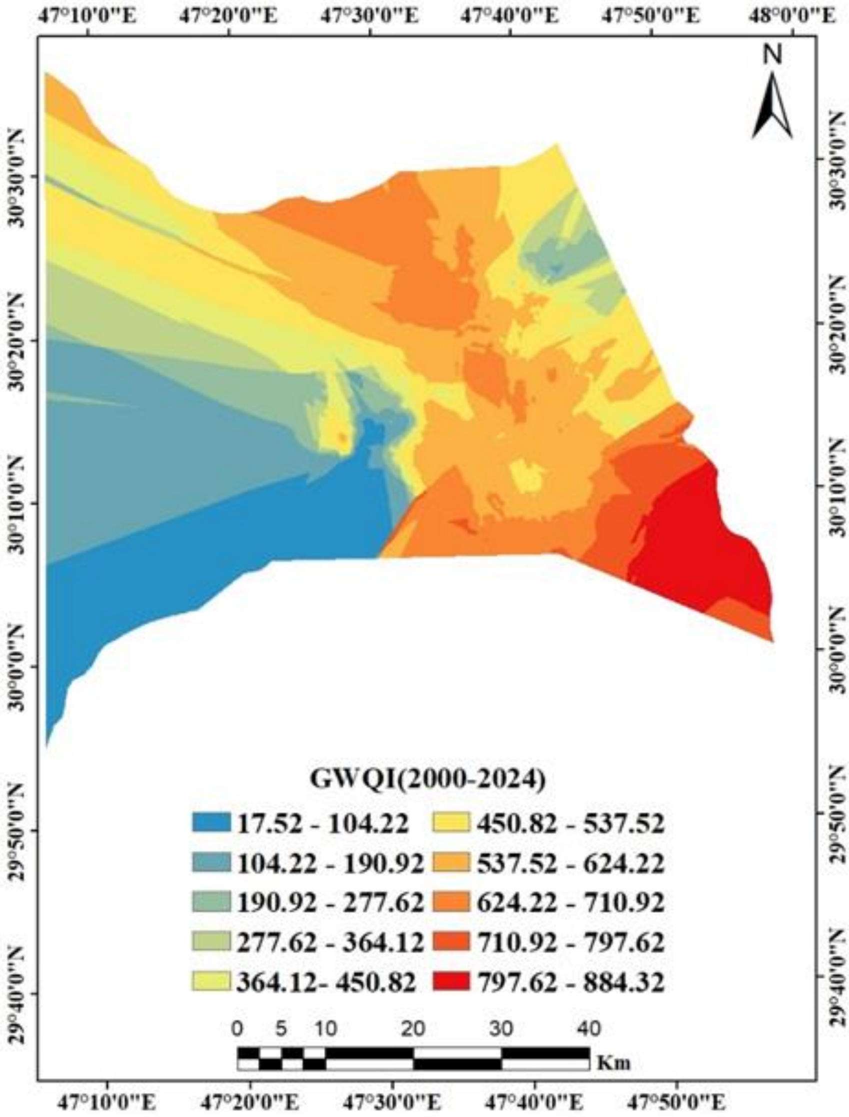

Fig. 12. The spatial distribution of GWQI (2000-2024)

Table 4. Results of information entropy and weight (2000–2007)

Parameter	P_{ij}	e_j	$1 - e_j$	W_{ij}
PH	1	1.133909261	-0.133909261	-0.279601771
EC	1	0.963288906	0.036711094	0.076652553
TDS	1	0.952830279	0.047169721	0.098490107
K^+	1	0.961739432	0.038260568	0.079887847
Ca^{2+}	1	0.919258256	0.080741744	0.1685883
Mg^{2+}	1	0.926582999	0.073417001	0.153294279
Na^+	1	0.977187466	0.022812534	0.047632439
Cl^-	1	0.953346938	0.046653062	0.097411327
HCO_3^-	1	0.983680434	0.016319566	0.034075161
NO_3^-	1	0.933628026	0.066371974	0.138584301
SO_4^{2-}	1	0.815619487	0.184380513	0.384985457

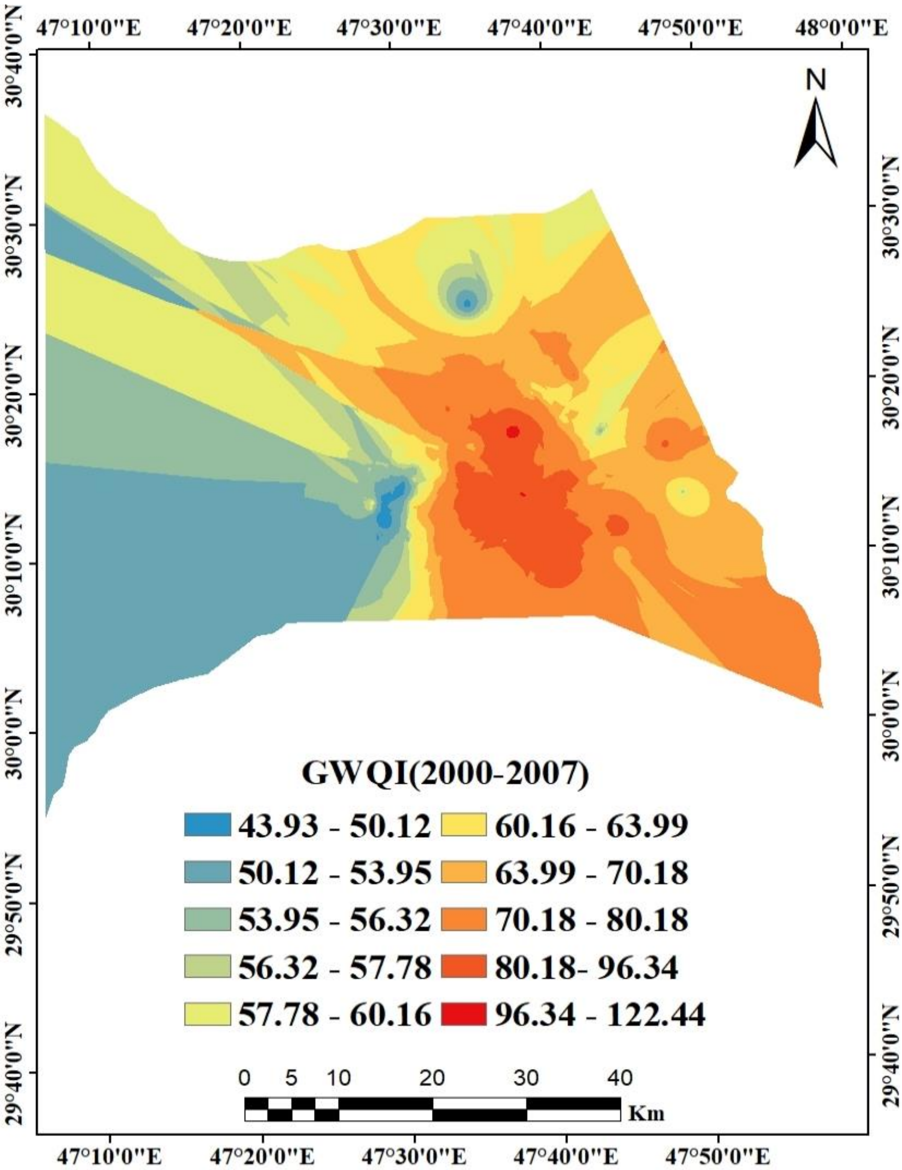

Fig. 13. The spatial distribution of GWQI (2000-2007)

Table 5. Results of information entropy and weight (2008–2015)

Parameter	P_{ij}	e_j	$1-e_j$	W_{ij}
PH	1	0.979295708	0.020458902	0.051694241
EC	1	0.937323865	0.062676135	0.15648906
TDS	1	0.975346854	0.024653146	0.061553694
K^+	1	0.968875389	0.031124611	0.077711573
Ca^{2+}	1	0.924796022	0.075203978	0.187768435
Mg^{2+}	1	0.953548581	0.046451419	0.115979373
Na^+	1	0.953737457	0.046262543	0.115507791
Cl^-	1	0.959801224	0.040198776	0.100367846
HCO_3^-	1	0.983573668	0.016426332	0.041013079
NO_3^-	1	0.974471083	0.025528917	0.063740309
SO_4^{2-}	1	0.988715665	0.011284335	0.0281746

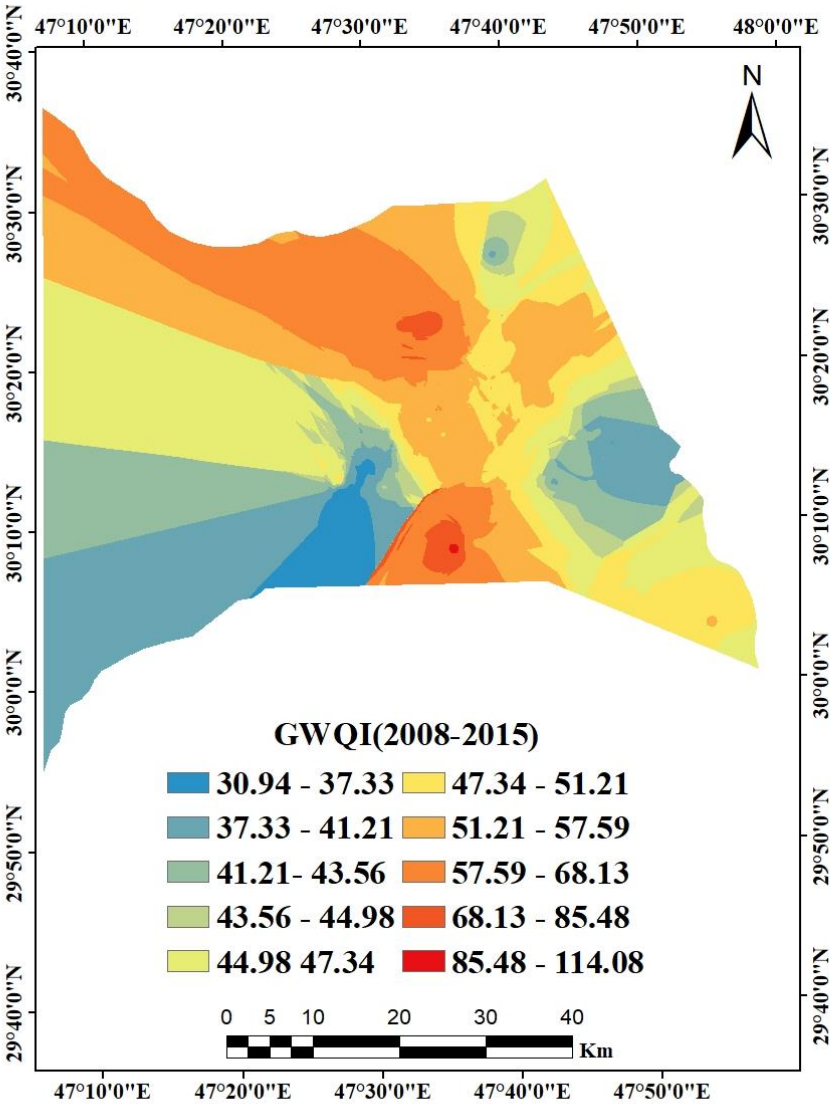

Fig. 14. The spatial distribution of GWQI (2008-2015)

Table 6. Results of information entropy and weight (2016–2024)

Parameter	P_{ij}	e_j	$1 - e_j$	W_{ij}
PH	1	1.546807455	-0.546807455	-0.658210126
EC	1	0.957024334	0.042975666	0.051731223
TDS	1	0.943630196	0.056369804	0.067854187
K^+	1	0.910844662	0.089155338	0.107319215
Ca^{2+}	1	0.889686643	0.110313357	0.132787817
Mg^{2+}	1	0.810085563	0.189914437	0.228606257
Na^+	1	0.794553601	0.205446399	0.247302591
Cl^-	1	0.919859087	0.080140913	0.096468254
HCO_3^-	1	0.905706334	0.094293666	0.113504389
NO_3^-	1	0.852461968	0.147538032	0.177596384
SO_4^{2-}	1	0.638591081	0.361408919	0.435039808

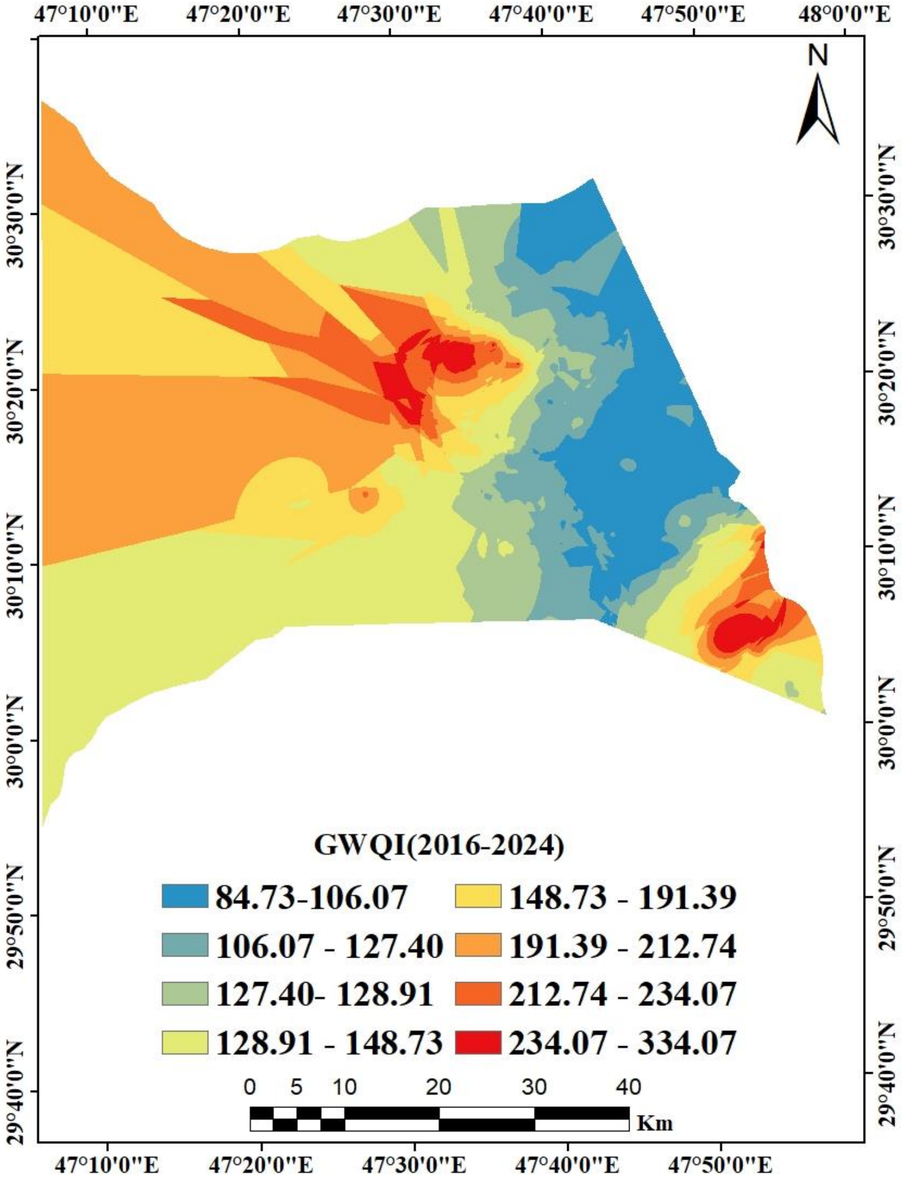

Fig. 15. The spatial distribution of GWQI (2016-2024)

5. Conclusions

Groundwater Quality Index (GWQI) analysis in the Dibdiba aquifer revealed clear spatial variation, with higher index values indicating poorer water quality found in the central, eastern, and southeastern parts of the study area. In contrast, lower GWQI values, indicating better water quality, were observed in the southwestern desert region, which represents a natural recharge zone. The improved quality in the southwest is attributed to minimal human activities, which reduces the risk of contamination. Over the 24-year study period, a marked overall decline in groundwater quality was detected. A moderate reduction of approximately 10% in water quality was observed between the first (2000-2007) and second (2008-2015) periods, followed by a sharp deterioration in the third period (2016-2024), as indicated by elevated GWQI values. This deterioration was primarily associated with increased concentrations of $So_4^{2-,}$ Cl^-, mg^{2+}, Na^+, and TDS. Based on the computed GWQI values and the classification criteria (0-50 = Excellent, 50-100 = Good, 100-200 = Poor, 200-300 = Very Poor, >300 = Unsuitable for drinking based on WHO, 2017 standards, most groundwater samples from the 2016–2024 period recorded values exceeding 300. This indicates that the water is unsuitable for direct human consumption and requires sustainable treatment. This observed decline is attributed to reduced annual rainfall, increasing abstraction rates, and the encroachment of saline water, especially in the southern parts of the study area. These findings highlight the urgent need for integrated water resource management and regular monitoring in arid and semi-arid environments.

Acknowledgements

The authors are very grateful to the reviewers for their outstanding efforts and valuable comments. Additionally, we extend our gratitude to the Basra branch of the Groundwater Authority for their helpful assistance.

References

Abdulameer, M.H., Al-Mallah, I.A., 2018. Evaluation of groundwater quality and the hydrogeochemical processes of shallow Dibdibba aquifer in Basra Governorate, southern Iraq. Journal of Basrah Researches (Sciences), 44(1). https://doi.org/10.1007/s11631-022-00549-8.

Al-Dulaimi, A.M.S., Al-Kubaisi, Q.Y., 2022. Hydrochemistry and water quality index of groundwater in Abu-Jir Village in Al-Anbar, Western Iraq. Iraqi Geological Journal, 55(2B), 73-84. https://doi.org/10.46717/igj.55.2B.7Ms-2022-08-23.

Al-Muslih, S.S., 2012. Hydrochemistry of the groundwater in Sha'abani-Bawara area, central west Iraq. Iraqi Bulletin of Geology and Mining, 8(1), 25-39.

Al-Ozeer, A.Z., Al-Abadi, A.M., 2022. Groundwater quality index assessment using the entropy method on the Nineveh plain in northern Iraq. Iraqi Geological Journal, 55(1A), 128-138. https://doi.org/10.46717/igj.55.1a.10ms-2022-01-29.

Al-Qurnawi, W.S., Alhawi, N.A., Alabadi, M.A., Al-Muhamed, R.A., 2024. Investigation of the hydrocarbon contamination of the Dibdibba aquifer in Al-Zubair area, southern Iraq. In Institute of Physics Publishing Conference Series: Earth and Environmental Science, 1300(1), 012023). https://doi.org/10.1088/1755-1315/1300/1/012023.

Al-Ramahi, F.K., Ali, A.B., Rasheed, M.J., 2024. Remote sensing of climatic factors and the spectral reflectivity and their impact on the morphological characteristics of the Al-Hammar Marsh. Iraqi Geological Journal, 57(2E), 292-311. https://doi.org/10.46717/igj.57.2e.21ms-2024-11-30.

Al-Sudani, H.I.Z., 2019. Groundwater system of Dibdibba sandstone aquifer in south of Iraq. Applied Water Science, 9(8), 72. https://doi.org/10.1007/s13201-019-0952-6.

Asadi, S.S., Vuppala, P., Reddy, M.A., 2007. Remote sensing and GIS techniques for evaluation of groundwater quality in municipal corporation of hyderabad (Zone-V), India. International Journal of Environmental Research and Public Health, 4(1), 45-52. doi:10.3390/ijerph2007010008.

Atiaa, A.M. 2000. Hydrogeology of Safwan-Zubair Area, South of Iraq. PhD thesis, College of Science, University of Basrah, Basrah.

Atiaa, A.M., Al-Asadiy, S.A.A.A., 2007. Management of groundwater resource of Dibdibba sandy aquifer in Safwan-Zubair area, south of Iraq. Journal of the College of Arts, 42, 200.

Awadh, S.M., Al-Kilabi, J.A., Abdulhussein, F.M., 2016. Assessment of groundwater quality using water quality index in Al-Hawija area, northern Iraq. Iraqi Geological Journal, 39-49(1), 67-76. https://doi.org/10.46717/igj.39-49.1.5Ms-2016-06-27.

Dwivedi, S.L., Pathak, V., 2007. A preliminary assignment of water quality index to Mandakini river, Chitrakoot. Indian Journal of Environmental Protection, 27, 1036-1038.

Fatah, K.K., Hamed, M., Saeed, M.H., Dara, R., 2020. Evaluation groundwater quality by using GIS and water quality index techniques for wells in Bardarash area, northern Iraq. Iraqi Geological Journal, 53(2C), 87-104. https://doi.org/10.46717/igj.53.2c.7Rs-2020-09.07.

Ghalib, H.B., 2008. Simulation study of the effect of artificial recharge on the water quality of shallow Dibdibba clastic aquifer in Zubair-Safwan area, south of Iraq. Journal Basrah Researches (Sciences), 34(4A), 47-49.

Jassim, S.Z., Goff, J.C., 2006. Geology of Iraq (2nd ed.). Dolin, Prague and Moravian Museum, Brno.

Pradhan, S.K., Patnaik, D., Rout, S.P., 2001. Water quality index for the groundwater around a phosphatic fertilizer plant. Indian Journal of Environmental Protection, 21(4), 355–358.

Reza, R., Singh, G., 2010. Heavy metal contamination and its indexing approach for river water. International Journal of Environmental Science and Technology, 7, 785-792. https://doi.org/10.1007/bf03326187.

Saeedi, M., Abessi, O., Sharifi, F., Meraji, H., 2010. Development of groundwater quality index (GWQI). Environmental Monitoring and Assessment, 163(1-4), 327-335. doi: 10.1007/s10661-009-0837-5.

Sahu, P., Sikdar, P.K., 2008. Hydrochemical framework of the aquifer in and around East Kolkata Wetlands, West Bengal, India. Environmental geology, 55, 823-835. https://doi.org/10.1007/s00254-007-1034-x.

Shi-fei, D., Zhong-zhi, S., 2005. Studies on incidence pattern recognition based on information entropy. Journal of Information Science, 31(6), 497-502. https://doi.org/10.1177/0165551505057012.

WHO, 2017. Guidelines for Drinking-Water Quality. Fourth Edition Incorporating the First Addendum.

Yashooa, N.K., Mawlood, D.K., Sissakian, V.K., 2024. Assessing water quality index in Kani-Qirzhala area, Erbil city, Kurdistan region of Iraq. Iraqi Geological Journal, 57(1D), 219-232. https://doi.org/10.46717/igj.57.1D.16ms-2024-4-26.

Yidana, S.M., Yidana, A., 2010. Assessing water quality using water quality index and multivariate analysis, Environmental Earth Sciences, 59(7), 1461–1473. doi: 10.1007/s12665-009-0132-3.

Yufeng, S., Fengxiang, J., 2009. Landslide stability analysis based on generalized information entropy. In the 2009 International Conference on Environmental Science and Information Application Technology, 2, 83-85. IEEE. https://doi.org/10.1109/etcs.2009.738.